

---

# Microbial Signatures in Metabolic Syndrome Individuals: A Distinct Intestinal Microbiota Composition Profile Prevails in People Living with HIV Compared to HIV-Negative Individuals

---

[Fernando Amador-Lara](#) , Verónica Rígggen-Bueno , [Jaime F. Andrade-Villanueva](#) , [Luz A. González-Hernández](#) , Karina Sánchez-Reyes , [Montserrat Álvarez-Zavala](#) , [Andrea Torres-Rojas](#) , Samuel E. Amador-Castro , [Miriam Ruth Bueno-Topete](#) \* , [Tonatiuh Abimael Baltazar-Díaz](#) \*

Posted Date: 8 May 2026

doi: 10.20944/preprints202605.0441.v1

Keywords: metabolic syndrome; chronic HIV infection; intestinal microbiota; dysbiosis



Preprints.org is a free multidisciplinary platform providing preprint service that is dedicated to making early versions of research outputs permanently available and citable. Preprints posted at Preprints.org appear in Web of Science, Crossref, Google Scholar, Scilit, Europe PMC, OpenAlex.

Copyright: This open access article is published under a [Creative Commons CC BY 4.0 license](#), which permit the free download, distribution, and reuse, provided that the author and preprint are cited in any reuse.

Disclaimer/Publisher's Note: The statements, opinions, and data contained in all publications are solely those of the individual author(s) and contributor(s) and not of MDPI and/or the editor(s). MDPI and/or the editor(s) disclaim responsibility for any injury to people or property resulting from any ideas, methods, instructions, or products referred to in the content.

Article

# Microbial Signatures in Metabolic Syndrome Individuals: A Distinct Intestinal Microbiota Composition Profile Prevails in People Living with HIV Compared to HIV-Negative Individuals

Fernando Amador-Lara <sup>1,2</sup>, Verónica Riggen-Bueno <sup>3</sup>, Jaime F. Andrade-Villanueva <sup>1,2,3</sup>, Luz A. González-Hernández <sup>1,2,3</sup>, Karina Sánchez-Reyes <sup>1,4</sup>, Monserrat Álvarez-Zavala <sup>1,4</sup>, Andrea Torres-Rojas <sup>4,5</sup>, Samuel E. Amador-Castro <sup>6</sup>, Miriam Ruth Bueno-Topete <sup>3,\*</sup> and Tonatiuh Abimael Baltazar-Díaz <sup>3,\*</sup>

<sup>1</sup> Departamento de Clínicas Médicas, Centro Universitario de Ciencias de la Salud, Universidad de Guadalajara, Guadalajara 44280, Mexico

<sup>2</sup> Unidad de VIH, Hospital Civil de Guadalajara Fray Antonio Alcalde, Guadalajara 44280, Mexico

<sup>3</sup> Instituto de Investigación en Enfermedades Crónicas Degenerativas, Departamento de Biología Molecular y Genómica, Centro Universitario de Ciencias de la Salud, Universidad de Guadalajara, Guadalajara 44340, Mexico

<sup>4</sup> Instituto de Investigación en Inmunodeficiencias y VIH, Centro Universitario de Ciencias de la Salud, Universidad de Guadalajara, Hospital 278, Guadalajara 44280, Mexico

<sup>5</sup> Programa de Doctorado en Ciencias en Biología Molecular, Centro Universitario de Ciencias de la Salud, Universidad de Guadalajara, Guadalajara 44340, México

<sup>6</sup> Licenciatura en Médico Cirujano y Partero, Centro Universitario de Ciencias de la Salud CUCS, Universidad de Guadalajara, Guadalajara 44340, Mexico

\* Correspondence: miriam.bueno@academicos.udg.mx (M.R.B.-T.); tonatiuh.baltazar@academicos.udg.mx (T.A.B.-D.)

## Abstract

Metabolic syndrome (MetS) is highly prevalent in people living with HIV (PLHIV), but whether their intestinal microbiota differs from that of HIV-negative individuals with MetS remains unclear. We conducted a cross-sectional study including 30 virologically suppressed PLHIV with MetS and 30 HIV-negative individuals with MetS. Fecal microbiota composition was assessed by 16S rRNA gene sequencing, and predicted functional profiles were inferred using PICRUSt2 and MetaCyc. PLHIV with MetS exhibited markedly reduced alpha diversity and a clearly distinct beta diversity profile compared with HIV-negative MetS, indicating a remodeled community structure. Differential abundance analysis showed enrichment in PLHIV + MetS of *Prevotella*, *Selenomonas*, *Odoribacter*, *Christensenellaceae* R-7 group, and uncultured *Lachnospiraceae*, whereas *Subdoligranulum* and the *Ruminococcus gausvreauii* group were relatively more abundant in HIV-negative MetS. Functional predictions revealed higher representation in PLHIV + MetS of Gram-negative cell envelope and lipopolysaccharide-related pathways, amino acid degradation, and ppGpp biosynthesis, while HIV-negative MetS showed comparatively greater saccharolytic potential. Carbohydrate-related pathways correlated positively with adiposity and blood pressure, and *Prevotella* correlated positively with BMI only in PLHIV + MetS. These findings support MetS in chronic treated HIV as a distinct dysbiotic and metabolically adverse intestinal phenotype and highlight the intestinal microbiota as a potential target for microbiome-oriented interventions in this population.

**Keywords:** metabolic syndrome; chronic HIV infection; intestinal microbiota; dysbiosis

## 1. Introduction

Metabolic syndrome (MetS) is a cluster of interrelated conditions – including central obesity, dyslipidemia (high triglycerides, low HDL cholesterol), hypertension, and hyperglycemia – that together markedly increase the risk of type 2 diabetes (T2D) and cardiovascular disease (CVD) [1]. Globally, MetS affects in a proportion of 12.5–31.4% of adults [2]. Individuals with MetS have substantially higher risk of CVD, T2D, certain cancers, and overall mortality [3]. MetS is characterized by persistent insulin resistance (IR) and a state of low-grade chronic inflammation, both of which represent fundamental pathophysiological features of the condition [4].

Epidemiological studies show that MetS is common in people living with HIV (PLHIV). Prevalence estimates among HIV-infected adults vary widely (often reported on the order of 10–40% depending on definition and population), but recent evidence suggests that HIV infection confers an increased risk of MetS compared to uninfected individuals [5]. In one systematic review and meta-analysis, HIV infection was associated with approximately 1.6-fold higher odds ratio of MetS relative to HIV-negative controls and antiretroviral therapy (ART) use further amplified this risk: patients receiving ART had roughly 1.5 times the risk of developing MetS as untreated patients [6]. In practice, the ageing of the PLHIV, combined with ART-associated metabolic side effects (especially weight gain reported with newer INSTI+TAF regimens), has led to an increasing burden of MetS among PLHIV. This is clinically important because MetS in the setting of HIV carries even greater consequences: PLHIV already has elevated cardiovascular risk due to persistent immune activation and ART toxicity [7]. Indeed, effective ART has transformed HIV into a chronic condition and shifted morbidity toward age-related noncommunicable diseases – including cardiovascular, metabolic, renal and hepatic disorders – which now occur at higher rates in PLHIV than in age-matched uninfected populations [8]. Chronic immune activation in HIV (the so-called “inflammaging” of treated PLHIV) means that even middle-aged PLHIV often display complications (CVD, MetS, neurocognitive decline) characteristic of older people [9]. In short, MetS substantially increases mortality risk in the general population [10], and in PLHIV this risk is compounded by HIV-specific inflammation and accelerated aging [11].

The intestinal microbiota has emerged as a key regulator of metabolic health and systemic inflammation. A healthy intestinal microbiome helps maintain the intestinal barrier and modulate immune responses, whereas intestinal dysbiosis (an imbalance in microbial composition) can promote metabolic and inflammatory disease [12]. Indeed, dysbiosis has been implicated in obesity, IR, T2D, hypertension and CVD [13]. Several studies have reported that individuals with MetS or related disorders exhibit distinct microbiome features (for example, reduced diversity and altered abundance of short-chain fatty acid-producing bacteria) [14]. In HIV-negative populations, metabolic disease has been consistently linked to shifts in intestinal bacterial composition [15]. Notably, one multi-omic study found that microbial translocation (a condition characterized by an increased intestinal permeability and elevated bacterial subproducts in blood) elevated lipopolysaccharide-binding protein, was a central predictor of impaired metabolic health, connecting intestinal microbiome alterations, diet, and inflammation to MetS [16]. Together these findings suggest that changes in intestinal microbiota are intimately involved in MetS pathogenesis. However, to date no single microbial “signature” of MetS has been robustly identified – much remains unknown about the specific taxa or functions that distinguish MetS patients from healthy controls, and particularly how HIV infection might modify those features.

HIV infection itself causes profound and often irreversible damage to intestinal mucosa and microbiota. During acute HIV infection, the virus targets intestinal-associated lymphoid tissue, depleting CD4<sup>+</sup> T cells and disrupting the epithelial barrier. This leads to microbial translocation (passage of bacterial products as lipopolysaccharide into the circulation) and a state of chronic immune activation [17]. Even with suppressive ART, many PLHIV have lingering dysbiosis – their intestinal microbial communities remain altered compared to uninfected individuals [18]. For example, ART-treated PLHIV often show decreased  $\alpha$ -diversity and enrichment of pro-inflammatory bacteria (e.g. Gammaproteobacteria) along with depletion of beneficial taxa (e.g. *Ruminococcaceae*) [8].

These HIV-associated alterations in the intestinal microbiota are thought to perpetuate systemic inflammation despite ART. Importantly, HIV-related factors such as sexual behavior, immune status, and ART regimen further shape the microbiome. Men who have sex with men (MSM) – a major HIV risk group – have a distinct microbiome signature (marked by *Prevotella* enrichment) linked to sexual practices [19].

HIV-related alterations of the intestine (from mucosal damage, immune activation, and behavioral factors) could lead to a different microbial configuration in MetS compared to HIV-seronegative individuals with MetS. Exploring these differences could reveal novel pathogenic mechanisms and targets. Therefore, the aim of this study was to characterize the intestinal microbiota composition and predict metabolic function in HIV-infected versus HIV-uninfected individuals with MetS. We hypothesized that PLHIV with MetS harbor a distinct intestinal microbial profile, reflecting the compounded effects of HIV-induced dysbiosis and metabolic dysregulation. By elucidating these differences, we seek to advance understanding of the microbial underpinnings of MetS in the context of HIV and to inform future interventions that target microbiota to improve inflammatory and metabolic outcomes in this population.

## 2. Materials and Methods

### 2.1. Study Design and Participants

We conducted a cross-sectional observational study involving 30 PLHIV diagnosed with MetS according to the 2005 NCEP-ATP III criteria. Participants were recruited from the HIV Unit at Hospital Civil de Guadalajara, Jalisco, Mexico. Additionally, 30 confirmed HIV-negative individuals with MetS were designed as control subjects. Recruitment was conducted between January 2019 and May 2024.

Inclusion criteria for PLHIV included adults aged 18–60 years, diagnosed with HIV for at least one year, on an INSTI-containing regimen for a minimum of 12 months, and with HIV viral load undetectable for at least six months. Exclusion criteria included pregnancy, lactation, active AIDS-defining illnesses, co-infection with hepatitis B or C, chronic renal or pancreatic disease, malabsorptive disorders, and recent use (within 30 days) of antibiotics, probiotics, prebiotics, corticosteroids, NSAIDs, immunosuppressants, or vitamin supplements.

The study adhered to the Ethical Principles for Medical Research Involving Human Subjects, with all procedures conducted in accordance with relevant guidelines and regulations, as outlined in the Declaration of Helsinki. The protocol was approved by the Ethics Committee of the Hospital Civil de Guadalajara (protocol code: n.061/19), and written informed consent was obtained from all participants prior to enrollment.

### 2.2. Laboratory Assessment

Blood samples were collected from all participants and sent at Central Laboratory of Civil Hospital of Guadalajara “Fray Antonio Alcalde”. Glucose and lipid profile were determined by colorimetric and photometric tests (AU5800 autoanalyzer, Coulter Beckman, USA). For viremic control and immunological status a blood sample in an EDTA-tube was obtained and sent to State Reference Laboratory, CD4<sup>+</sup> T-cells count was measured by flow cytometry (FACScalibur System, Becton Dickinson) and HIV-1 viral load was determined using with real-time polymerase chain reaction with retro transcription (Cobas AmpliPrep/Cobas Taqman, Roche Diagnostics).

### 2.3. Anthropometric and Clinical Assessment

Measurements were taken in the morning after an overnight fast. Weight and height were recorded using a calibrated Seca 700 scale and stadiometer. Waist circumference was measured in triplicate midway between the lowest rib and iliac crest; hip circumference was measured at the widest point of the buttocks. BMI was classified according to WHO criteria. All patients completed a

face-to-face validated semi-quantitative food frequency questionnaire, and a 24-h dietary recall (24HR) through the Nutricloud® digital system.

#### 2.4. DNA Extraction and 16S rRNA Sequencing

Faecal samples were collected and immediately stored at  $-80^{\circ}\text{C}$ . DNA was extracted from 150 mg of frozen faeces using Quick-DNA Fecal/Soil Microbe Miniprep Kit (Zymo Research, Irvine, CA, USA) according to the manufacturer's protocol. DNA was quantified with NanoDrop™ OneC spectrophotometer (Thermo Scientific, Waltham, MA, USA) and purity using the A260/280 ratio was also revised. The 16S rRNA amplicon sequencing library preparation was performed according to Illumina MiSeq System's protocol [20]. The V3 and V4 regions of the 16S rRNA gene were amplified using PCR following the manufacturer's protocol with Platinum Taq DNA Polymerase High Fidelity (Invitrogen, Waltham, MA, USA) and previously published primers: 341F: 5'TCGTCGGCAGCGTCAGATGTGTATAAGAGACAGCCTACGGGNGGCWGCAG-3' and 805R: 5'GTCTCGTGGGCTCGGAGATGTGTATAAGAGACAGGACTACHVGGGTATCTAATCC-3'. Obtained amplicons were further purified with AMPure XP (Beckman Coulter, Indianapolis, IN, USA) magnetic beads and quantified with the Qubit 3 dsDNA HS kit (Invitrogen, Waltham, MA, USA) according to manufacturer's indications. Index incorporation was achieved with the Nextera XT Index Kit v2 Set A (Illumina, San Diego, CA, USA). Finally, indexed amplicons were pooled to equimolar concentrations into a 4 nmol/L solution tube. The resulted library was denatured and further sequenced using the MiSeq Reagent V3 600-cycle (Illumina, San Diego, CA, USA) according to protocol.

#### 2.5. Bioinformatic and Statistical Analyses

Analysis of 16S rRNA sequences were performed with QIIME2 version 2024.2 *amplicon* distribution [21]. Sequences whose Phred  $\geq 30$  (quality parameter) were accepted. 3,343,914 reads in 60 samples were further filtered by denoising with DADA2 via *q2-dada2* [22] at default settings. A total of 1,318,263 biological features (amplicon sequence variants or ASVs) across 60 samples were obtained. Taxonomy assignment was performed trained on our own data using a naïve classifier (*via q2-feature-classifier*) [23], employing Silva 138.1 as a reference taxonomic database [24,25]. ASVs identified as mitochondria and chloroplasts were removed. Then, filtered ASVs were aligned using MAFFT via *q2-alignment* [26], and phylogeny was built with FastTree2 via *q2-phylogeny* [26]. Alpha diversity indices [27–29] and beta diversity distances (unweighted and weighted Unifrac, [30,31]) were computed via *q2-diversity*. PCoA plots were generated to visualize beta diversity distances using Emperor via *q2-emperor* [32] and further analyzed PERMANOVA. Effects of different variables on beta diversity were determined using Adonis Permutational Multivariate Analysis of Variance via *q2-diversity adonis*.

Differential abundance analyses were accomplished by means of ANCOM-BC (*via q2-composition*), which is a compositional statistical method that accounts for sampling fraction and normalize read counts, while controlling false discovery rates [33]. ANCOM-BC plugin incorporates a false discovery rate (FDR) method to correct the *p*-values for multiple testing (*q*-value). Before analysis, a frequency filter was applied in which features that appeared more than 50 times in at least 10% of the samples were retained. A  $q \leq 0.05$  cut-off was used to assess significance, and a log fold change (LFC)  $\geq |1.0|$  to assess the effect size. To assess the potential metabolic profile of the intestinal microbiota, PICRUSt2 pipeline [34–38] was employed, coupled with the MetaCyc Database [39]. The resulting pathways were further analyzed using ANCOM-BC, using a frequency filter which retained features that appeared more than 500 times in at least 10% of the samples, with a  $q \leq 0.05$  and a LFC  $\geq |1.0|$ . Pseudomonadota/Bacillota (also known as Proteobacteria/Firmicutes) ratio was calculated as previously published [40]. Core microbiome taxa at genus level and MetaCyc pathways identified by PICRUSt2 for both study groups were identified using the *q2-core-features* plugin. For taxa, a minimum fraction of 0.9 and a maximum fraction of 1.0; for MetaCyc pathways, we employed a threshold of 0.99 and 1.0. These data were used to identify shared potential taxa and

predicted pathways which were later employed to calculate Spearman correlations. These correlations were calculated using centered log-ratio (clr) transformed counts.

Data normality was examined using the D'Agostino-Pearson omnibus test. If significant, a parametric distribution was assumed and unpaired Student's t-test or one-way ANOVA with a Bonferroni *post hoc* test was performed to assess the differences between the groups; if not, the Mann-Whitney U or Kruskal-Wallis with a Dunn's *post hoc* test was performed. Beta diversity distances were statistically analyzed by performing PERMANOVA tests. Both alpha and beta diversity statistical analyses were corrected with Benjamini-Hochberg (BH) multiple testing through QIIME2 package. The Fisher's exact test was applied to evaluate categorical variables. All statistical tests were two-tailed, and a *p*-value or false discovery rate-adjusted *q*-value equal to or less than 0.05 were considered statistically significant. Data were analyzed using SPSS 25.0, unless otherwise specified. Plots were generated utilizing GraphPad Prism version 9.0.0.

### 3. Results

#### 3.1. Clinical and Demographic Characteristics

A total of 60 participants were analyzed (thirty participants in the MetS group and thirty in the PLHIV + MetS group). No significant differences were found in mean age or sex distribution. Furthermore, the MetS group showed a significantly higher mean weight (110.45 kg vs. 89.9 kg, *p* = 0.002) compared to the PLHIV + MetS group, as well as BMI (35.55 vs. 30.95 kg/m<sup>2</sup>, *p* < 0.001). PLHIV + MetS showed significantly higher LDL-C levels. Other anthropometric measures and metabolic indices did not show significant differences (Table 1). No differences in caloric intake were observed between groups based on the 24-hour dietary recall or the semi-quantitative food frequency questionnaire.

**Table 1.** Sociodemographic and clinical characteristics of recruited participants.

	MetS (seronegative to HIV) n=30	PLHIV + MetS n=30	<i>p</i>
Age (years)	38.96 ± 11.58	42.80 ± 10.18	0.179 <sup>b</sup>
Biological sex			
Female	14	7	0.103 <sup>c</sup>
Male	16	23	
Current smoking	7 (23)	9 (30)	0.386 <sup>c</sup>
Current alcohol	12 (40)	15 (50)	0.302
Illicit drug use	0 (0)	0 (0)	NA
Receptive anal intercourse	10 (33.3)	18 (60)	0.069
Physical activity (>30 min, ≥3 times per week)	6 (20)	9 (30)	0.276
Weight (kg)	110.45 (86.65-135.45)	89.9 (79.88-98.28)	0.002 <sup>a</sup>
Height (m)	1.69 (1.59-1.79)	1.735 (1.66-1.76)	0.982 <sup>a</sup>
BMI (kg/m <sup>2</sup> )	35.55 (33.3-42.68)	30.95 (28.78-32.74)	<0.001 <sup>a</sup>
BMI ranges			
Normal weight	0	3	0.001 <sup>c</sup>
Overweight	0	10	
Obese class I	13	14	
Obese class II	7	3	
Obese class III	10	0	
Waist circumference (cm)	100.5 (88.75-107.75)	101.25 (93.08-107.63)	0.433 <sup>a</sup>
Visceral adiposity index	4.11 (2.53-5.79)	3.84 (2.49-6.28)	0.882 <sup>a</sup>
Waist-to-height ratio	57.81 (54.65-62.52)	60.16 (54.72-63.37)	0.344 <sup>a</sup>
Glucose (mg/dL)	101.5 (92-107.75)	96 (86-107)	0.239 <sup>a</sup>
Total cholesterol (mg/dL)	151.5 (131.25-176.25)	166 (151.75-200.25)	0.053 <sup>a</sup>
HDL-c (mg/dL)	35 (27.75-38)	31 (28-35)	0.142 <sup>a</sup>

LDL-c (mg/dL)	72.5 (57.75-91)	102.5 (86.25-128.5)	<0.001 <sup>a</sup>
Triglycerides (mg/dL)	204 (182.5-269.25)	192 (120.5-267.75)	0.158 <sup>a</sup>
Triglycerides/HDL-c ratio	6.50 (4.31-9.02)	5.47 (3.99-8.76)	0.605 <sup>a</sup>
Mean arterial blood pressure (mmHg)	108 (99.83-115.75)	87 (77-87.25)	<0.001 <sup>a</sup>
Systolic blood pressure	137 (129-150.25)	119.5 (110-120.5)	<0.001 <sup>a</sup>
Diastolic blood pressure	94 (86.75-99.25)	70 (60-70)	<0.001 <sup>a</sup>
Absolute T CD4 <sup>+</sup> (cell count/ $\mu$ L)	NA	682.76 $\pm$ 232.91	NA
Nadir T CD4 <sup>+</sup> (cell count/ $\mu$ L)	NA	436.03 $\pm$ 301.18	NA
Time since HIV diagnosis (years)	NA	6 (2-12.25)	NA
Duration of ART (years)	NA	3 (2-10)	NA
Time of INSTI use (years)	NA	2 (1-2)	NA
HIV-1 RNA (copies/mL)	NA	40 (20-50)	NA

Abbreviations: MetS: metabolic syndrome patients, PLHIV + MetS: people living with HIV plus metabolic syndrome, BMI: body mass index, HDL-c: High-density lipoprotein cholesterol, LDL-c: Low-density lipoprotein cholesterol, ART: Antiretroviral therapy, INSTI: integrase strand-transfer inhibitor group, NA: not applicable. Data are shown as mean  $\pm$  standard deviation or median with interquartile range in parentheses. *p* values were calculated by (°) Mann-Whitney U test, (°) Student's *t*-test, (°) square Chi test.

### 3.2. Alpha Diversity

Alpha diversity metrics were used to assess microbial richness and evenness. We found significantly reduced alpha diversity in the PLHIV + MetS group compared to the HIV-negative MetS group, as indicated by lower values in observed features ( $p < 0.0001$ ), Chao1 richness estimator ( $p < 0.0001$ ), and Shannon diversity index ( $p < 0.001$ ) (Figure 1).

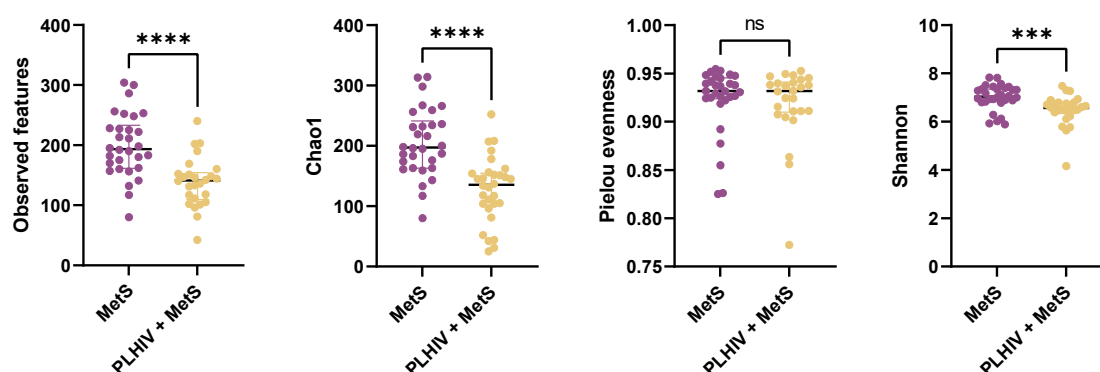


**Figure 1.** Intestinal microbiota alpha diversity metrics. These metrics evaluate richness, diversity, underrepresented taxa and evenness of the MetS and PLHIV + MetS groups. Data were statistically analyzed using the Mann-Whitney U test. Median and interquartile ranges are shown in black lines. ns = not significant, \*\*\* =  $p < 0.001$ , \*\*\*\* =  $p < 0.0001$ .

### 3.3. Beta Diversity

Richness and diversity indices, such as observed features, Shannon, and Chao1 showed a significant loss of richness and diversity in PLHIV + MetS group ( $p < 0.001$ , Figure 1). However, no differences were observed between both groups when evenness was assessed using the Pielou index. Regarding beta diversity, the principal coordinates analysis (PCoA) revealed well-defined clusters, consistent with a significant difference in the intestinal microbiota profile between the two groups ( $q < 0.001$ ) using the unweighted and weighted Unifrac metrics (Figure 2), clearly indicating that these are two distinct profiles between PLHIV + MetS and MetS groups. Likewise, a greater distance (assessed through pseudo-F) was observed between the two groups using the weighted Unifrac metric than with the unweighted Unifrac metric (Table 2). The weighted Unifrac metric assesses quantitative aspects of beta diversity, while the unweighted Unifrac metric assesses qualitative

aspects. Moreover, we performed an Adonis analysis to determine the effects of other variables on beta diversity in both groups, such as age ranges, BMI, BMI ranges, and biological sex. The first statistical model ruled out the significant influence of age range and biological sex on beta diversity, as assessed by both Unifrac metrics (Supplementary Table 1). Consequently, the second model considered the primary grouping variable (PLHIV + MetS and MetS) and BMI as a continuous variable, confirming that both variables interact significantly (Supplementary Table 2). Finally, we modeled the effect of BMI in each group independently. These tests showed that in the PLHIV + MetS group, BMI also significantly influences beta diversity, as assessed by the weighted Unifrac metric; however, no significant influence was observed in the unweighted Unifrac metric (Supplementary Table 3). Notably, in the MetS group (seronegative to HIV), BMI did not show significant influence on beta diversity using any metric (Supplementary Table 4). Consequently, we infer that body composition assessed through BMI is a covariate with a significant influence on intestinal microbiota composition in the PLHIV + MetS group, with a negligible effect in the seronegative group.

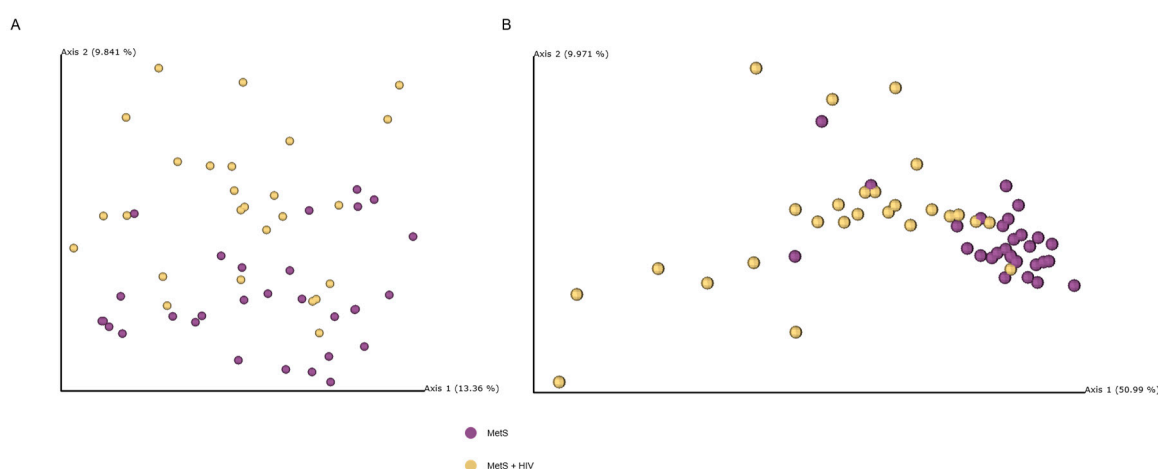


**Figure 2.** Beta diversity PCoA plots for unweighted (left) and weighted Unifrac (right) distances in the MetS (purple) and PLHIV + MetS (gold) groups.

**Table 2.** PERMANOVA analysis results for unweighted and weighted Unifrac distances.

Group 1	Group 2	Pseudo-F	q-value
Unweighted Unifrac			
MetS	PLHIV + MetS	3.03	0.001
Weighted Unifrac			
MetS	PLHIV + MetS	16.68	0.001

### 3.4. Relative Abundance at Different Taxonomic Levels

At the phylum level, an increase in the relative abundance of the phylum *Bacillota* was observed in the MetS group compared to the PLHIV + MetS group (88.2% vs 62.7%). On the other hand, a clear increase in the relative abundances of the phyla *Bacteroidota* (28.5% vs 7.5%) and *Pseudomonadota* (4.7% vs 1.6%) was shown in the PLHIV + MetS group, compared to the MetS group, as observed in Figure 3 (left). Conversely, at the genus level, a marked increase in the relative abundance of *Prevotella* was observed in the PLHIV + MetS group, which was accompanied by an increase in *Blautia* in the MetS group (Figure 3, right). Other taxa, such as *Lachnospiraceae*, *Faecalibacterium*, *Agathobacter* and *Roseburia* showed a slight increase in the MetS group, compared to the PLHIV + MetS group.

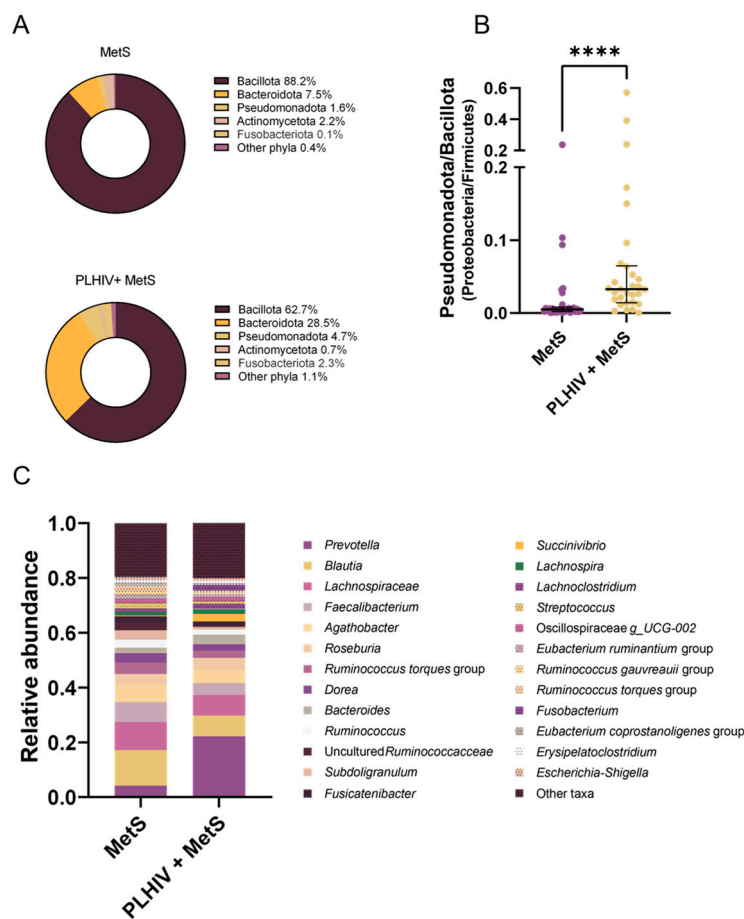


**Figure 3.** Relative bacterial abundances across phylum and genus levels and *Pseudomonadota/Bacillota* (*Proteobacteria/Firmicutes*) ratio in the groups MetS and PLHIV + MetS. (A) Donut chart represents main phyla in both groups, accompanied by relative abundance percentages. Top 5 phyla are shown, while minor phyla are summarized into the other phyla category. (B) *Pseudomonadota/Bacillota* (also called *Proteobacteria/Firmicutes*) ratio. Values closer to 1 indicate a greater relative abundance of *Pseudomonadota*, while values closer to 0 indicate a greater abundance of *Bacillota*. Results are showed as mean  $\pm$  SEM (standard error of the mean). \*\*\*\*  $p < 0.0001$  (C) Stacked barplot of bacterial genera in both groups. Top 25 taxa (ordered by median) are depicted, minor taxa are summarized into the other taxa category.

### 3.5. Differential Abundance of Bacterial Taxa

Regarding the differential taxonomic abundance analysis, performed by ANCOM-BC (Figure 4), it showed a clear enrichment in *Prevotella*, *Selenomonas*, *Odoribacter*, *Christensenellaceae* R-7 and uncultured *Lachnospiraceae* in the PLHIV + MetS group ( $q < 0.0001$ ,  $LFC \leq 1.8$ ); likewise, other taxa such as *Parabacteroides*, *Weisella* ( $q < 0.001$ ) *Butyrivibrio* and the *Eubacterium oxidoreducens* group ( $q < 0.05$ ) were also characteristic of this group. On the other hand, the *Ruminococcus gauvreauii* group and the *Subdoligranulum* genus distinguished the MetS group, although they do not reach statistical significance.

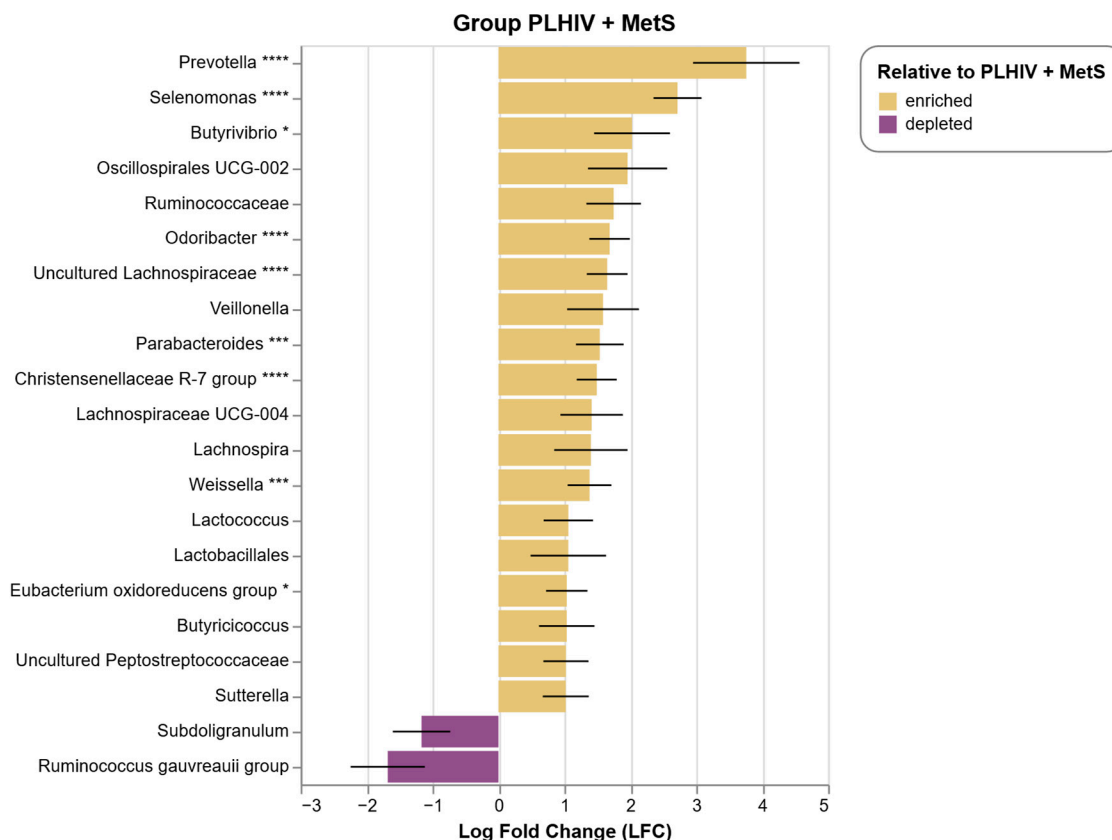


**Figure 4.** Differentially abundant taxa in the MetS and PLHIV + MetS groups determined by ANCOM-BC. Bars length depicts log fold change (LFC) between both groups and black lines stand for standard error. A threshold of  $LFC \geq |1.0|$  was applied. Gold bars represent taxa enriched in the PLHIV + MetS group, whereas purple bars account for depleted taxa (that is, enriched in the MetS group). \* =  $q < 0.05$ , \*\*\* =  $q < 0.001$ , \*\*\*\* =  $q < 0.0001$ .

### 3.6. Functional Pathway Predictions

The functional potential profiles of the sequenced communities were predicted using PICRUSt2 and MetaCyc database (figure 5 and supplementary figure 1). In the PLHIV + MetS group, we found different pathways mainly related to the synthesis of components associated with the bacterial wall of Gram-negative species e.g., lipid IVA biosynthesis (NAGLIPASYN-PWY), ketodeoxyoctonate biosynthesis (PWY-6467 and PWY-1269) anhydromuropeptides recycling PWY0-1261, degradation of L-tyrosine (TYRFUMCAT-PWY, log fold change [lfc] 2.56,  $q < 0.0001$ ), L-leucine (LEU-DEG2-PWY, lfc 2.43,  $q < 0.0001$ ), L-histidine (PWY-5028, lfc 1.59,  $q < 0.01$ ), and aromatic biogenic amine (PWY-7431), plus synthesis of bacterial alarmones, such as ppGpp. On the other hand, MetS group exhibited increased pathways for saccharolytic fermentation such as lactose and galactose degradation (LACTOSECAT-PWY, lfc -1.42,  $q < 0.05$ ) or glycerol fermentation to butanol (PWY-7003, lfc -1.20,  $q < 0.05$ ).

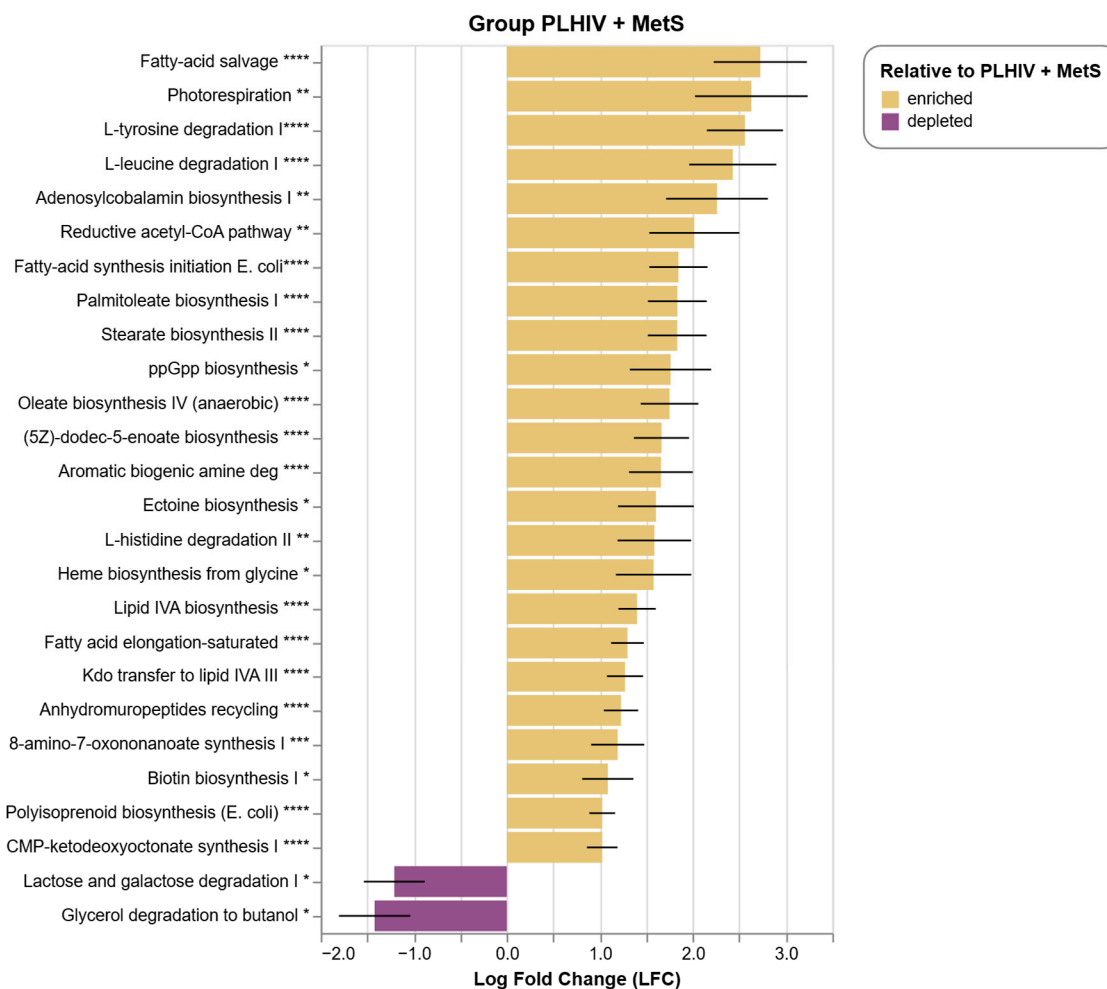


**Figure 5.** Differential metabolic pathways predicted by PICRUSt2 in the MetS and PLHIV + MetS groups, analyzed by ANCOM-BC. A threshold of LFC  $\geq |1.0|$  was applied. Gold bars represent pathways enriched in the PLHIV + MetS group, whereas purple bars account for depleted pathways (that is, enriched in the MetS group). \* =  $q < 0.05$ , \*\* =  $q < 0.01$ , \*\*\*\* =  $q < 0.0001$ .

### 3.7. Core Taxa, Predicted Metabolic Pathways and Correlation Analysis

To identify shared taxa and predicted bacterial pathways among both groups, and to calculate further correlations between common taxa, bacterial pathways and metabolic parameters measured in both groups, core analyses and correlations were performed. We found that in 90% of the samples, the core microbiome were Gram-positive anaerobes such as *Erysipelatoclostridium*, *Blautia*, *Dorea*, *Faecalibacterium*, among others (supplementary figure 2 and supplementary table 5). On the other hand, the core-features analysis revealed that in 100% of the samples, 174 metabolic pathways were shared in both groups (supplementary figure 3, supplementary table 6). Among these, we found very interesting pathways that point to bacterial carbohydrate metabolism, such as glycogen synthesis and degradation (GLYCOGENSYNTH-PWY and GLYCOCAT-PWY), as well as sucrose (PWY-621) and starch (PWY-6737) degradation.

Considering these shared metabolic taxa and pathways, positive correlations were calculated between *Erysipelatoclostridium*, *Blautia*, *Dorea*, and *Faecalibacterium* with BMI, MAP, SBP, DBP, and body fat percentage. Notably, *Erysipelatoclostridium* correlated negatively with total cholesterol, whereas *Dorea* and *Faecalibacterium* correlated negatively with LDL-c and lean mass percentage (Figure 6 and supplemental figures S4 and S5). Interestingly, *Prevotella* correlated positively with BMI ( $\rho=0.506$ ,  $p<0.01$ ), but only in the PLHIV + MetS group. Also, weak but significant inverse correlations were found between *Prevotella* and mean arterial pressure ( $\rho=-0.256$ ,  $p<0.05$ ) and DBP ( $\rho=-0.263$ ,  $p<0.05$ ) in all participants. On the other hand, glycogen synthesis and degradation pathways, as well

as sucrose and starch degradation pathways, correlated positively with parameters such as BMI, MAP, and body fat percentage, whereas a negative correlation was observed with lean mass percentage. Finally, sucrose and starch degradation pathways correlated negatively with LDL-c levels. Nevertheless, glycogen synthesis and degradation pathways also showed a positive correlation with LDL-c.

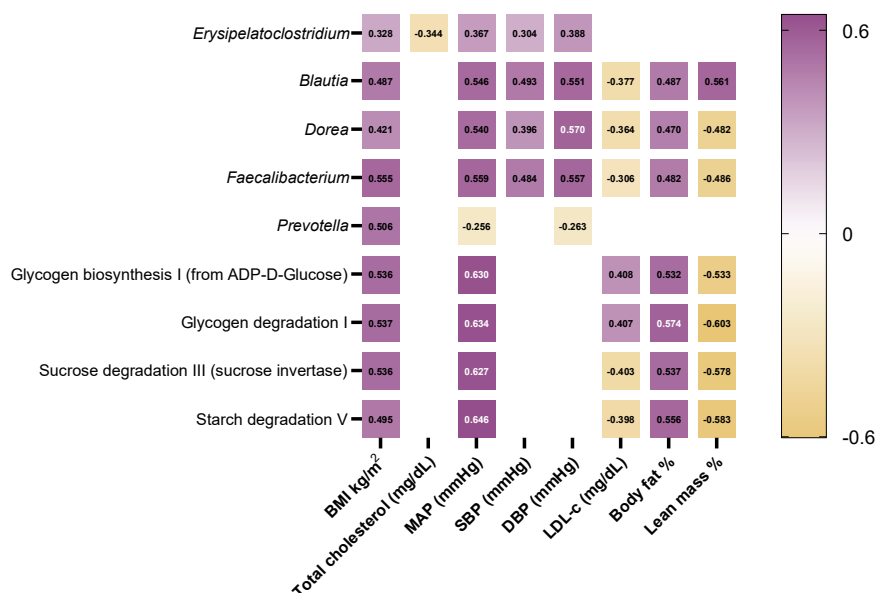


**Figure 6.** Correlation matrix between metabolic parameters, core taxa and MetaCyc pathways shared in MetS and PLHIV + MetS groups. Correlations were calculated using the Spearman test, using a color scale (purple, positive correlation; yellow, negative correlation). Taxa and MetaCyc pathway counts were previously clr-transformed. Significance threshold is  $p < 0.05$ . BMI: body mass index, MAP: mean arterial blood pressure, SBP: systolic blood pressure, DBP: diastolic blood pressure, LDL-c: Low-density lipoprotein cholesterol.

#### 4. Discussion

This study provides evidence that PLHIV + MetS harbors a distinct intestinal microbiota profile compared with HIV-negative individuals with MetS. Overall, the findings support the concept that HIV infection, even under suppressive ART and with relatively preserved CD4<sup>+</sup> T-cell counts, is associated with reduced microbial diversity, taxonomic remodeling, and predicted functional shifts toward inflammatory and proteolytic metabolism. This interpretation is consistent with current evidence showing that treated HIV remains associated with persistent microbiome disruption, incomplete restoration of intestinal homeostasis, and links to noncommunicable comorbidities [8,41–43].

A major finding was the significantly lower alpha diversity observed in the PLHIV + MetS group. Reduced richness and diversity are among the most consistent signatures of HIV-associated dysbiosis and have been linked to microbial translocation, systemic immune activation, and metabolic impairment [8,41–44]. In this context, reduced diversity has been independently associated with metabolic complications, including IR and dyslipidemia, among PLHIV [8]. The persistence of this pattern despite virologic suppression reinforces the concept that intestinal ecosystem disruption remains a chronic feature of treated HIV infection [18]. Because lower microbial diversity has also been associated with adverse cardiometabolic phenotypes, this observation may help explain part of the excess metabolic risk in PLHIV [8,15,18].

Beta diversity analysis further showed a clear ecological separation between PLHIV + MetS and HIV-negative individuals with MetS. The difference was evident with both unweighted and weighted UniFrac metrics, indicating that HIV-related microbial remodeling affects not only rare taxa

but also the overall relative abundance structure of the community. These data support the view that MetS in PLHIV is not merely the metabolic counterpart of MetS in HIV-negative people, but rather a distinct microbiological phenotype shaped by HIV-associated mucosal injury, immune dysregulation, and ART exposure [8,18,41–43].

Through differential abundance analysis, we identified distinct bacterial genera enriched or depleted in the PLHIV + MetS group compared to MetS. Notably, *Prevotella* was significantly enriched among PLHIV. *Prevotella* dominance has been extensively reported in this population, particularly in men who have sex with men (MSM), and is often associated with increased pro-inflammatory signaling and microbial translocation [44]. Some *Prevotella* species, such as *P. copri* has a wide genomic and functional variability at the strain level that allows it to adapt to the type of nutrients available in the intestine, while some strains can degrade fibers from diets rich in fruits and vegetables and produce short-chain fatty acid (SCFAs) [45], others to synthesize branched-chain amino acids from meat-rich diets [46,47]. Conversely, other *Prevotella* species behave as pathobionts, for instance, *P. intestinalis* has been associated with intestinal inflammation and metabolic alterations due to reduced SCFA production [48].

In PLHIV, *Prevotella* abundance has been positively correlated with elevated IL-18 [49], a cytokine that increases intestinal permeability and epithelial cell death *in vitro* [50], accompanied by higher fatty acid-binding protein (I-FABP) and IL-18 serum levels, especially in individuals with hypertriglyceridemia [51,52]. Interestingly, *Prevotella* spp. abundance was higher in PLHIV with CD4<sup>+</sup> counts >350 cells/ $\mu$ L, consistent with our cohort, suggesting that microbial dysbiosis may persist despite immune recovery [53]. A recent study also found a positive correlation between *Prevotella* and BMI, further implicating its role in metabolic risk [54]. Our results align with these findings, where we determined that *Prevotella* positively correlates with BMI ( $\rho=0.506$ ,  $p<0.01$ ) in PLHIV + MetS group; notably, this correlation was not found in MetS group. A recent multi-omics study integrating metabolomic, lipidomic, and fecal microbiota data from PLHIV under long-term suppressive ART revealed that a metabolically high-risk profile was strongly associated with *Prevotella* enrichment, systemic inflammation, and increased prevalence of MetS [55]. These findings underscore the relevance of microbiome composition in shaping cardiometabolic outcomes in this population.

The enrichment of *Selenomonas* in PLHIV + MetS is also noteworthy. *Selenomonas*, a genus comprising Gram-negative anaerobic bacteria, species of which have been isolated from the oral cavity and are frequently associated with periodontal disease [56]. Previous studies have described increases in *Selenomonas* in the oral microbiota of PLHIV, which increases according to the duration of antiretroviral therapy [57,58]. Thus, it is possible that the enrichment of *Selenomonas* in PLHIV + MetS may reflect a compromised mucosal integrity and immune dysfunction that permits translocation of oral taxa to the intestinal tract. This finding aligns with broader evidence that HIV can disrupt the gut-oral microbiome axis and facilitate displacement of oral-associated taxa into the intestinal compartment [54].

Similarly, we found an increased abundance of *Butyrivibrio* and uncultured *Lachnospiraceae* in PLHIV + MetS. Although typically considered beneficial SCFA producers, the ecological roles of these taxa in a dysbiotic HIV-infected intestinal remain unclear. This apparently mixed environment, where SCFA producers are incremented along with proinflammatory bacteria, such as *Prevotella* and *Proteobacteria* members has been previously described by our research group in PLHIV with a normal BMI (18.5–24.9 kg/m<sup>2</sup>), without metabolic comorbidities, under the same ART regimen and duration [40].

In addition, the rise in *Parabacteroides* and *Odoribacter*, both SCFA producers with mixed associations in health and disease, might reflect selective pressures unique to HIV-associated dysbiosis [59]. This expansion in SCFA-producing bacteria, mainly butyrogenic, has already been documented in other cohorts of PLHIV [59–61], suggesting probable compensatory mechanisms in response to inflammation or changes in substrate availability [62]. However, this apparent compensatory response implies an increase in butyrogenic bacteria that are not part of the intestinal

microbiota of HIV- individuals, which is mirrored by an abnormal butyrate production that may be synthesized by non-canonical pathways [40].

In contrast, the HIV-negative MetS group showed relatively greater representation of taxa commonly associated with a more favorable anaerobic intestinal ecosystem, including *Blautia*, *Faecalibacterium*, *Agathobacter*, and *Roseburia*. In addition, *Subdoligranulum* and the *Ruminococcus gauvreauii* group were relatively more represented in HIV-negative MetS. These taxa are generally associated with carbohydrate fermentation, short-chain fatty acid production, and epithelial homeostasis [63–65]. Their relative depletion in PLHIV + MetS may therefore be clinically meaningful because butyrate-producing bacteria have been linked to lower microbial translocation, reduced inflammation, and improved intestinal barrier function in HIV [66,67]. This pattern supports the idea that HIV amplifies the loss of microbial groups associated with mucosal and metabolic resilience [66–68]. Herein, more recent work has linked the loss of these taxa in PLHIV to accelerated biological aging [69]

*Ruminococcus gauvreauii* is a commensal bacterium involved in the fermentation of host-indigestible polysaccharides, notably producing acetate. Although less characterized than other intestinal commensals, decrease in its abundance has been associated with advanced coronary artery disease, independent of traditional risk factors [70]. Likewise, *Subdoligranulum*, another key butyrate-producing genus, was depleted in PLHIV + MetS, and enriched in HIV- with MetS. Interestingly, a decreased abundance of this genus has been associated with MetS and dyslipidemia in Romanian population [71]. Higher relative abundance of *Subdoligranulum* has been linked to favorable lipid profiles, including elevated HDL cholesterol, and inversely associated with multiple metabolic risk markers such as C-reactive protein, fatty liver index, insulin resistance (HOMA-IR), and HbA1c [55]. In the population of western Mexico, our group has determined that *Subdoligranulum* is one of the key genera of the intestinal microbiota of clinically healthy patients [72,73]. Moreover, therapeutic interventions including metformin and acarbose have been shown to increase the abundance of *Subdoligranulum* in fecal microbiota [64], further suggesting that its presence is associated with beneficial effects, although it does not imply causality [74]

The functional predictions derived from PICRUST2 reinforce these compositional findings. PLHIV + MetS showed enrichment in pathways related to Gram-negative cell envelope synthesis, lipopolysaccharide-related metabolism including lipid IVA biosynthesis, ketodeoxyoctonate biosynthesis, and anhydromuropeptide recycling, and amino acid degradation including strong enrichment of L-tyrosine, L-leucine, and L-histidine. Although these inferences require confirmation by shotgun metagenomics and metabolomics, these pathways are often carried by Gram-negative taxa such as *Enterobacteriaceae* and *Pseudomonadaceae*, whose overrepresentation has been reported in HIV-associated dysbiosis [18]. An increased LPS biosynthetic potential is clinically relevant, as people living with HIV have chronically elevated plasma LPS levels even on therapy, contributing to monocyte activation and systemic inflammation [75]. Notably, LPS-driven endotoxemia is implicated in adipose inflammation and IR [76], suggesting that the enrichment of LPS-related lipids biosynthesis pathways in PLHIV + MetS could exacerbate metabolic inflammation. Likewise, increased proteolytic metabolism leads to the production of branched-chain fatty acids and aromatic metabolites (e.g., imidazole propionate), which impair insulin signaling and promote metabolic inflammation [77,78]. Intriguingly, a recent review on HIV and cardiometabolic comorbidities noted that the intestinal microbiome of PLHIV exhibits reduced capacity for beneficial SCFA production and increased levels of microbially-derived metabolites like imidazole propionate [79]. Our findings strongly align with this pattern. Imidazole propionate has been shown to inhibit insulin signaling via activation of the mTORC1 pathway and has been found elevated in both T2D and MetS [80].

Although our study did not directly measure microbial metabolites, the overrepresentation of amino acid degradation pathways in PLHIV + MetS is consistent with the hypothesis that HIV-associated dysbiosis may amplify cardiometabolic risk through metabolite-mediated mechanisms and reduced metabolic responsiveness [77–80].

A broader view of the MetaCyc results suggests that the functional differences between groups reflect reprogramming rather than complete replacement of the metabolic background associated with MetS. Several carbohydrate-related pathways, including glycogen synthesis/degradation and sucrose and starch degradation, were highly prevalent in both groups and formed part of the shared core pathway profile. This observation suggests that a substantial portion of the functional microbiome is conserved across MetS regardless of HIV status. However, the relative weighting of specific modules differed, with PLHIV + MetS showing stronger enrichment of pathways linked to Gram-negative envelope biosynthesis and proteolytic metabolism, whereas the HIV-negative MetS group retained relatively more saccharolytic functions, including lactose/galactose degradation and glycerol fermentation to butanol. This pattern suggests a more carbohydrate-oriented microbial metabolism than that observed in PLHIV + MetS [81–85]. However, this should not be interpreted simplistically as uniformly beneficial. In obesity and MetS, saccharolytic activity and short-chain fatty acid-related signatures may reflect both adaptive and maladaptive host-microbe interactions depending on substrate availability, microbial context, and host metabolic state [81]. From a biological perspective, these data suggest that HIV does not replace the metabolic framework of MetS but rather redirects it toward a more inflammatory and ecologically unstable configuration [15,79,81–85].

The observed correlations between taxa, predicted pathways, and clinical variables provide additional context for these interpretations. Positive associations between *Blautia*, *Dorea*, *Faecalibacterium*, and adiposity or blood pressure parameters illustrate that genus-level identities alone may not be sufficient to infer metabolic effects, especially in the setting of MetS [73–77]. Likewise, the inverse association between *Prevotella* and blood pressure in the overall cohort could reflect strain-level heterogeneity or metabolite-specific effects, including propionate-related signaling pathways known to influence blood pressure regulation [56,78,79]. Therefore, taxonomic patterns should be interpreted in conjunction with functional context rather than in isolation.

The observed correlations between taxa, predicted pathways, and clinical variables provide additional context for these interpretations. At the taxonomic level, positive associations between *Blautia*, *Dorea*, and *Faecalibacterium* with adiposity or blood pressure parameters illustrate that genus-level identities alone may not be sufficient to infer metabolic effects, especially in the setting of MetS [83,86–89]. Shared carbohydrate-related pathways correlated positively with BMI, body fat percentage, and mean arterial pressure, while glycogen-related pathways were also associated with LDL-c suggesting that some microbiome-metabolic relationships may be common to MetS itself [63,81–85]. In parallel, *Prevotella* correlated positively with BMI only in PLHIV + MetS. These findings suggest that some microbiome-metabolic relationships may be common to MetS itself, whereas others become context-dependent in the presence of chronic treated HIV infection. Likewise, the inverse association between *Prevotella* and blood pressure in the overall cohort could reflect strain-level heterogeneity or metabolite-specific effects, including propionate-related signaling pathways known to influence blood pressure regulation [63,86,87]. They also reinforce the importance of interpreting taxonomic patterns together with their functional context rather than in isolation and support the concept that greater fermentative or SCFA-related microbial potential is not necessarily synonymous with metabolic benefit, since obesity and MetS have repeatedly been associated with elevated fecal SCFAs and altered saccharolytic signatures in the context of dysbiosis and cardiometabolic risk [63,81–85]. Therefore, taxonomic patterns should be interpreted in conjunction with functional context rather than in isolation.

Taken together, the findings support the idea that HIV-associated metabolic dysbiosis persists despite virologic control and acceptable CD4+ T-cell recovery. This has potential clinical implications because routine HIV monitoring may not fully capture the biological burden associated with cardiometabolic comorbidity. The intestinal microbiota may represent an intermediate phenotype linking ART exposure, mucosal immune activation, diet, and long-term metabolic risk [18,49,55,68]. These data also suggest that microbiome-directed interventions, including dietary modulation,

prebiotics, probiotics, or future targeted microbial therapeutics, could be relevant adjunctive strategies in PLHIV + MetS [80,84].

A major strength of this study is the direct comparison between PLHIV and HIV-negative individuals matched for the presence of MetS, allowing the microbial component linked specifically to HIV infection to be assessed within a metabolically relevant context. The use of 16S rRNA sequencing, compositional differential abundance analysis, predicted functional inference, and correlation with detailed metabolic phenotypes provided a layered overview of the microbiome-host interaction. In addition, the cohort was clinically well characterized and restricted to virologically suppressed PLHIV receiving INSTI-based ART, reducing confounding from uncontrolled HIV replication.

This study has several limitations. First, its cross-sectional nature prevents causal inference between HIV status, microbiota alterations, and metabolic outcomes. Longitudinal studies are required to determine temporal relationships and mechanistic links. Second, although we adjusted for potential confounders such as age and ART duration, residual confounding—particularly from diet, physical activity, or sexual practices—may remain. Body composition, assessed using body mass index, was shown to be a collinear covariate with the PLHIV + MetS and MetS groups, making it impossible to adjust for the independent effect of this variable. However, subsequent analyses suggest that body composition has a greater effect on intestinal microbiota composition in PLHIV + MetS patients compared to seronegative MetS patients. Dietary intake was recorded, but quantitative nutrient analysis was not incorporated into the statistical models. Third, 16S rRNA gene sequencing provides only genus-level taxonomic resolution and inferred functions, limiting functional accuracy. Validation using shotgun metagenomics and/or metabolomics would enhance interpretation. Fourth, the sample size, though sufficient to detect key differences, may not reflect the broader variability of microbiota in diverse HIV-positive populations. Lastly, although all PLHIV had virological suppression and CD4<sup>+</sup> counts >350 cells/μL, ART regimens, immune recovery trajectories, and comorbidities were not stratified and could influence results.

Despite these limitations, our results support the concept that HIV-associated dysbiosis may contribute to a distinct cardiometabolic intestinal microenvironment in PLHIV with MetS and justify longitudinal multi-omics studies to clarify causality and identify microbiome-linked therapeutic targets [18,49,79], with larger numbers of participants that allow discrimination of the effect of body composition.

## 5. Conclusions

In conclusion, people living with HIV and metabolic syndrome exhibit a distinct intestinal microbiota profile compared with HIV-negative individuals with metabolic syndrome, characterized by lower microbial diversity, taxonomic differences, and predicted functional shifts toward Gram-negative cell-envelope biosynthesis, lipopolysaccharide-related pathways, and amino acid degradation, whereas HIV-negative individuals retained relatively greater saccharolytic microbial potential. These findings suggest that, even under suppressive antiretroviral therapy, chronic treated HIV infection is associated with a persistent dysbiotic intestinal ecosystem superimposed on the metabolic syndrome background. Although the cross-sectional design and 16S-based functional prediction preclude causal inference, the intestinal microbiota may represent a relevant biological link between treated HIV infection and metabolic comorbidity. These findings support the concept that MetS in chronic treated HIV represents a specific dysbiotic and metabolically adverse phenotype that may contribute to cardiometabolic risk and highlight the intestinal microbiota as a plausible target for future microbiome-oriented interventions in this population.

**Supplementary Materials:** The following supporting information can be downloaded at the website of this paper posted on Preprints.org, Supplementary Figure S1: Waterfall plot of log fold change of absolute counts for differentially PICRUSt2 outputs, in terms of MetaCyc database pathways; Supplementary Figure S2: Core microbiome analysis which shows shared taxa between MetS and PLHIV + MetS; Supplementary table 1: Adonis

tests for testing the effect of several covariables in beta diversity distances; Supplementary table 2: Adonis tests for testing the interaction of BMI and Group variables; Supplementary table 3: Adonis tests for testing the effect BMI as a continuous variable in PLHIV + MetS group; Supplementary table 4: Adonis tests for testing the effect BMI as a continuous variable in MetS group; Supplementary Table 5: Core microbiome analysis showing the list of core taxa identified and their total percentile frequencies; Supplementary Figure S3: Core analysis which shows shared pathways between MetS and PLHIV + MetS; Supplementary Table 6: Core analysis showing the list of MetaCyc pathways identified and their total percentile frequencies; Supplementary Figure S4: Spearman correlations between identified core taxa and metabolic, anthropometric and clinical parameters in the MetS and PLHIV + MetS groups; Supplementary Figure S5: Spearman correlations between identified core MetaCyc pathways and metabolic, anthropometric and clinical parameters in the MetS and PLHIV + MetS groups.

**Author Contributions:** For research articles with several authors, a short paragraph specifying their individual contributions must be provided. The following statements should be used “Conceptualization, F.A.-L., M.R.B.-T., and T.A.B.-D.; methodology, F.A.-L., J.F.A.-V., L.A.G.-H. and M.R.B.-T.; software, T.A.B.-D.; validation, F.A.-L., V.R.-B., K.S.-R., M.A.-Z., A.T.-R. and T.A.B.-D.; formal analysis, F.A.-L., and T.A.B.-D.; investigation, F.A.-L., V.R.-B., J.F.A.-V., S.E.A.-C.; resources, J.F.A.-V., L.A.G.-H., M.R.B.-T. and T.A.B.-D.; data curation, F.A.-L., V.R.-B., S.E.A.-C.; writing—original draft preparation, F.A.-L. and T.A.B.-D.; writing—review and editing, F.A.-L., V.R.-B., J.F.A.-V., L.A.G.-H., K.S.-R., M.A.-Z., A.T.-R., M.R.B.-T. and T.A.B.-D.; visualization, F.A.-L. and T.A.B.-D.; supervision, M.R.B.-T. and T.A.B.-D.; project administration, M.R.B.-T. and T.A.B.-D., S.E.A.-C.; funding acquisition, F.A.-L., J.F.A.-V., L.A.G.-H., K.S.-R., M.R.B.-T., and T.A.B.-D. All authors have read and agreed to the published version of the manuscript.

**Funding:** This research received no external funding.

**Institutional Review Board Statement:** The study was conducted in accordance with the Declaration of Helsinki and approved by the Ethics Committee of the Hospital Civil de Guadalajara (protocol code n.061/19, date of approval 18-Jun-2019 for studies involving humans).

**Informed Consent Statement:** Informed consent was obtained from all subjects involved in the study.

**Data Availability Statement:** The datasets generated and analyzed during the current study are available in the SRA repository (PRJNA1306328): <http://www.ncbi.nlm.nih.gov/bioproject/1306328>.

**Conflicts of Interest:** The authors declare no conflicts of interest.

## References

1. Obeidat, A.A.; Ahmad, M.N.; Ghabashi, M.A.; Alazzeh, A.Y.; Habib, S.M.; Abu Al-Haijaa, D.; Azzeh, F.S. Developmental Trends of Metabolic Syndrome in the Past Two Decades: A Narrative Review. *J. Clin. Med.* 2025, *14*, 2402, doi:10.3390/jcm14072402.
2. Peterseim, C.M.; Jabbour, K.; Kamath Mulki, A. Metabolic Syndrome: An Updated Review on Diagnosis and Treatment for Primary Care Clinicians. *J. Prim. Care Community Health* 2024, *15*, doi:10.1177/21501319241309168.
3. Zhang, Z.; Pang, Y.; Shen, J.; Chen, W.; Hao, C.; Lei, Z. The New Definition of Metabolic Syndrome Including Hyperuricemia Improves Its Prognostic Value: Results from NHANES Database. *BMC Cardiovasc. Disord.* 2025, *25*, 93, doi:10.1186/s12872-025-04529-7.
4. Islam, Md.S.; Wei, P.; Suzauddula, M.; Nime, I.; Feroz, F.; Acharjee, M.; Pan, F. The Interplay of Factors in Metabolic Syndrome: Understanding Its Roots and Complexity. *Molecular Medicine* 2024, *30*, 279, doi:10.1186/s10020-024-01019-y.
5. Asgedom, Y.S.; Kebede, T.M.; Gebrekidan, A.Y.; Koyira, M.M.; Azeze, G.A.; Lombebo, A.A.; Efa, A.G.; Haile, K.E.; Kassie, G.A. Prevalence of Metabolic Syndrome among People Living with Human Immunodeficiency Virus in Sub-Saharan Africa: A Systematic Review and Meta-Analysis. *Sci. Rep.* 2024, *14*, 11709, doi:10.1038/s41598-024-62497-y.

6. Trachunthong, D.; Tipayamongkholgul, M.; Chumseng, S.; Darasawang, W.; Bundhamcharoen, K. Burden of Metabolic Syndrome in the Global Adult HIV-Infected Population: A Systematic Review and Meta-Analysis. *BMC Public Health* 2024, 24, 2657, doi:10.1186/s12889-024-20118-3.
7. Obare, L.M.; Temu, T.; Mallal, S.A.; Wanjalla, C.N. Inflammation in HIV and Its Impact on Atherosclerotic Cardiovascular Disease. *Circ. Res.* 2024, 134, 1515–1545, doi:10.1161/CIRCRESAHA.124.323891.
8. Vujkovic-Cvijin, I.; Sortino, O.; Verheij, E.; Sklar, J.; Wit, F.W.; Kootstra, N.A.; Sellers, B.; Brenchley, J.M.; Ananworanich, J.; Loeff, M.S. van der; et al. HIV-Associated Gut Dysbiosis Is Independent of Sexual Practice and Correlates with Noncommunicable Diseases. *Nat. Commun.* 2020, 11, 2448, doi:10.1038/s41467-020-16222-8.
9. Nasi, M.; De Biasi, S.; Gibellini, L.; Bianchini, E.; Pecorini, S.; Bacca, V.; Guaraldi, G.; Mussini, C.; Pinti, M.; Cossarizza, A. Ageing and Inflammation in Patients with HIV Infection. *Clin. Exp. Immunol.* 2016, 187, 44–52, doi:10.1111/cei.12814.
10. Li, J.; Liu, W.; Li, H.; Ye, X.; Qin, J.-J. Changes of Metabolic Syndrome Status Alter the Risks of Cardiovascular Diseases, Stroke and All Cause Mortality. *Sci. Rep.* 2025, 15, 5448, doi:10.1038/s41598-025-86385-1.
11. Sheets, K.; Baker, J. V HIV and Inflamm-Aging: How Do We Reach the Summit of Healthy Aging? *Top. Antivir. Med.* 2024, 32, 589–596.
12. Mostafavi Abdolmaleky, H.; Zhou, J.-R. Gut Microbiota Dysbiosis, Oxidative Stress, Inflammation, and Epigenetic Alterations in Metabolic Diseases. *Antioxidants* 2024, 13, 985, doi:10.3390/antiox13080985.
13. Amador-Lara, F.; Andrade-Villanueva, J.F.; Vega-Magaña, N.; Peña-Rodríguez, M.; Alvarez-Zavala, M.; Sanchez-Reyes, K.; Toscano-Piña, M.; Peregrina-Lucano, A.A.; del Toro-Arreola, S.; González-Hernández, L.A.; et al. Gut Microbiota from Mexican Patients with Metabolic Syndrome and HIV Infection: An Inflammatory Profile. *J. Appl. Microbiol.* 2022, 132, 3839–3852, doi:10.1111/jam.15505.
14. Fusco, W.; Lorenzo, M.B.; Cintoni, M.; Porcari, S.; Rinninella, E.; Kaitsas, F.; Lener, E.; Mele, M.C.; Gasbarrini, A.; Collado, M.C.; et al. Short-Chain Fatty-Acid-Producing Bacteria: Key Components of the Human Gut Microbiota. *Nutrients* 2023, 15, 2211, doi:10.3390/nu15092211.
15. Li, R.; Kurilshikov, A.; Yang, S.; van Oortmerssen, J.A.E.; van Hilten, A.; Ahmadizar, F.; Roshchupkin, G.; Kraaij, R.; Duijts, L.; Fu, J.; et al. Association between Gut Microbiome Profiles and Host Metabolic Health across the Life Course: A Population-Based Study. *The Lancet Regional Health - Europe* 2025, 50, 101195, doi:10.1016/j.lanepe.2024.101195.
16. Armstrong, A.J.S.; Quinn, K.; Fouquier, J.; Li, S.X.; Schneider, J.M.; Nusbacher, N.M.; Doenges, K.A.; Fiorillo, S.; Marden, T.J.; Higgins, J.; et al. Systems Analysis of Gut Microbiome Influence on Metabolic Disease in HIV-Positive and High-Risk Populations. *mSystems* 2021, 6, doi:10.1128/mSystems.01178-20.
17. Xiao, Q.; Yu, F.; Yan, L.; Zhao, H.; Zhang, F. Alterations in Circulating Markers in HIV/AIDS Patients with Poor Immune Reconstitution: Novel Insights from Microbial Translocation and Innate Immunity. *Front. Immunol.* 2022, 13, doi:10.3389/fimmu.2022.1026070.
18. Gáspár, Z.; Nagavci, B.; Szabó, B.G.; Lakatos, B. Gut Microbiome Alteration in HIV/AIDS and the Role of Antiretroviral Therapy—A Scoping Review. *Microorganisms* 2024, 12, 2221, doi:10.3390/microorganisms12112221.
19. Huang, K.D.; Amend, L.; Gálvez, E.J.C.; Lesker, T.-R.; de Oliveira, R.; Bielecka, A.; Blanco-Míguez, A.; Valles-Colomer, M.; Ruf, I.; Pasolli, E.; et al. Establishment of a Non-Westernized Gut Microbiota in Men Who Have Sex with Men Is Associated with Sexual Practices. *Cell Rep. Med.* 2024, 5, 101426, doi:10.1016/j.xcrm.2024.101426.
20. Illumina Inc. Illumina 16S Metagenomic Sequencing Library; 2013;
21. Bolyen, E.; Rideout, J.R.; Dillon, M.R.; Bokulich, N.A.; Abnet, C.C.; Al-Ghalith, G.A.; Alexander, H.; Alm, E.J.; Arumugam, M.; Asnicar, F.; et al. Reproducible, Interactive, Scalable and Extensible Microbiome Data Science Using QIIME 2. *Nat. Biotechnol.* 2019, 37, 852–857, doi:10.1038/s41587-019-0209-9.
22. Callahan, B.J.; McMurdie, P.J.; Rosen, M.J.; Han, A.W.; Johnson, A.J.A.; Holmes, S.P. DADA2: High-Resolution Sample Inference from Illumina Amplicon Data. *Nat. Methods* 2016, 13, 581–583, doi:10.1038/nmeth.3869.

23. Bokulich, N.A.; Kaehler, B.D.; Rideout, J.R.; Dillon, M.; Bolyen, E.; Knight, R.; Huttley, G.A.; Gregory Caporaso, J. Optimizing Taxonomic Classification of Marker-Gene Amplicon Sequences with QIIME 2's Q2-Feature-Classifer Plugin. *Microbiome* 2018, 6, 90, doi:10.1186/s40168-018-0470-z.
24. Robeson, M.S.; O'Rourke, D.R.; Kaehler, B.D.; Ziemski, M.; Dillon, M.R.; Foster, J.T.; Bokulich, N.A. *RESCRIPt: Reproducible Sequence Taxonomy Reference Database Management*; 2021; Vol. 17; ISBN 1111111111.
25. Glöckner, F.O.; Yilmaz, P.; Quast, C.; Gerken, J.; Beccati, A.; Ciuprina, A.; Bruns, G.; Yarza, P.; Peplies, J.; Westram, R.; et al. 25 Years of Serving the Community with Ribosomal RNA Gene Reference Databases and Tools. *J. Biotechnol.* 2017, 261, 169–176, doi:10.1016/j.jbiotec.2017.06.1198.
26. Katoh, K.; Misawa, K.; Kuma, K.I.; Miyata, T. MAFFT: A Novel Method for Rapid Multiple Sequence Alignment Based on Fast Fourier Transform. *Nucleic Acids Res.* 2002, 30, 3059–3066, doi:10.1093/nar/gkf436.
27. Shannon, C.E. A Mathematical Theory of Communication. *The Bell system technical journal* 1948, 27, 379–423.
28. Chao, A. Nonparametric Estimation of the Number of Classes in a Population. *Scandinavian Journal of Statistics* 1984, 11, 265–270.
29. Pielou, E.C. The Measurement of Diversity in Different Types of Biological Collections. *J. Theor. Biol.* 1966, 13, 131–144, doi:10.1016/0022-5193(66)90013-0.
30. Lozupone, C.; Knight, R. UniFrac: A New Phylogenetic Method for Comparing Microbial Communities. *Appl. Environ. Microbiol.* 2005, 71, 8228–8235, doi:10.1128/AEM.71.12.8228-8235.2005.
31. Lozupone, C.A.; Hamady, M.; Kelley, S.T.; Knight, R. Quantitative and Qualitative  $\beta$  Diversity Measures Lead to Different Insights into Factors That Structure Microbial Communities. *Appl. Environ. Microbiol.* 2007, 73, 1576–1585, doi:10.1128/AEM.01996-06.
32. Vázquez-Baeza, Y.; Pírrung, M.; Gonzalez, A.; Knight, R. EMPeror: A Tool for Visualizing High-Throughput Microbial Community Data. *Gigascience* 2013, 2, 16, doi:10.1186/2047-217X-2-16.
33. Lin, H.; Peddada, S. Das Analysis of Compositions of Microbiomes with Bias Correction. *Nat. Commun.* 2020, 11, 1–11, doi:10.1038/s41467-020-17041-7.
34. Douglas, G.M.; Maffei, V.J.; Zaneveld, J.R.; Yurgel, S.N.; Brown, J.R.; Taylor, C.M.; Huttenhower, C.; Langille, M.G.I. PICRUSt2 for Prediction of Metagenome Functions. *Nat. Biotechnol.* 2020, 38, 685–688, doi:10.1038/s41587-020-0548-6.
35. Barbera, P.; Kozlov, A.M.; Czech, L.; Morel, B.; Darriba, D.; Flouri, T.; Stamatakis, A. EPA-NG: Massively Parallel Evolutionary Placement of Genetic Sequences. *Syst. Biol.* 2019, 68, 365–369, doi:10.1093/sysbio/syy054.
36. Czech, L.; Barbera, P.; Stamatakis, A. Genesis and Gappa: Processing, Analyzing and Visualizing Phylogenetic (Placement) Data. *Bioinformatics* 2020, 36, 3263–3265, doi:10.1093/bioinformatics/btaa070.
37. Louca, S.; Doebeli, M. Efficient Comparative Phylogenetics on Large Trees. *Bioinformatics* 2018, 34, 1053–1055, doi:10.1093/bioinformatics/btx701.
38. Ye, Y.; Doak, T.G. A Parsimony Approach to Biological Pathway Reconstruction/Inference for Genomes and Metagenomes. *PLoS Comput. Biol.* 2009, 5, e1000465, doi:10.1371/journal.pcbi.1000465.
39. Caspi, R.; Altman, T.; Billington, R.; Dreher, K.; Foerster, H.; Fulcher, C.A.; Holland, T.A.; Keseler, I.M.; Kothari, A.; Kubo, A.; et al. The MetaCyc Database of Metabolic Pathways and Enzymes and the BioCyc Collection of Pathway/Genome Databases. *Nucleic Acids Res.* 2014, 42, D459–D471, doi:10.1093/nar/gkt1103.
40. Baltazar-Díaz, T.A.; Andrade-villanueva, J.F.; Paulina, S.Á.; Amador-lara, F.; Holgu, T.; Karina, S.; Monserrat, Á.; Bueno-topete, M.R.; Alicia, L. A Two-Faced Gut Microbiome: Butyrogenic and Proinflammatory Bacteria Predominate in the Intestinal Milieu of People Living with HIV from Western Mexico. *Int. J. Mol. Sci.* 2024, 25, doi:10.3390/ijms25094830.
41. Vujkovic-Cvijin, I.; Dunham, R.M.; Iwai, S.; Maher, M.C.; Albright, R.G.; Broadhurst, M.J.; Hernandez, R.D.; Lederman, M.M.; Huang, Y.; Somsouk, M.; et al. Dysbiosis of the Gut Microbiota Is Associated with HIV Disease Progression and Tryptophan Catabolism. *Sci. Transl. Med.* 2013, 5, 193ra91, doi:10.1126/scitranslmed.3006438.
42. Lozupone, C.A.; Li, M.; Campbell, T.B.; Flores, S.C.; Linderman, D.; Gebert, M.J.; Knight, R.; Fontenot, A.P.; Palmer, B.E. Alterations in the Gut Microbiota Associated with HIV-1 Infection. *Cell Host Microbe* 2013, 14, 329–339, doi:10.1016/j.chom.2013.08.006.

43. Gootenberg, D.B.; Paer, J.M.; Luevano, J.-M.; Kwon, D.S. HIV-Associated Changes in the Enteric Microbial Community: Potential Role in Loss of Homeostasis and Development of Systemic Inflammation. *Curr. Opin. Infect. Dis.* 2017, *30*, 31–43, doi:10.1097/QCO.0000000000000341.
44. Noguera-Julian, M.; Rocafort, M.; Guillén, Y.; Rivera, J.; Casadellà, M.; Nowak, P.; Hildebrand, F.; Zeller, G.; Parera, M.; Bellido, R.; et al. Gut Microbiota Linked to Sexual Preference and HIV Infection. *EBioMedicine* 2016, *5*, 135–146, doi:10.1016/j.ebiom.2016.01.032.
45. Meiners, F.; Kreikemeyer, B.; Newels, P.; Zude, I.; Walter, M.; Hartmann, A.; Palmer, D.; Fuellen, G.; Barrantes, I. Strawberry Dietary Intervention Influences Diversity and Increases Abundances of SCFA-Producing Bacteria in Healthy Elderly People. *Microbiol. Spectr.* 2025, *13*, doi:10.1128/spectrum.01913-24.
46. Abdelsalam, N.A.; Hegazy, S.M.; Aziz, R.K. The Curious Case of *Prevotella Copri*. *Gut Microbes* 2023, *15*, doi:10.1080/19490976.2023.2249152.
47. Ley, R.E. Gut Microbiota in 2015: *Prevotella* in the Gut: Choose Carefully. *Nat. Rev. Gastroenterol. Hepatol.* 2016, *13*, 69, doi:10.1038/nrgastro.2016.4.
48. Iljazovic, A.; Roy, U.; Gálvez, E.J.C.; Lesker, T.R.; Zhao, B.; Gronow, A.; Amend, L.; Will, S.E.; Hofmann, J.D.; Pils, M.C.; et al. Perturbation of the Gut Microbiome by *Prevotella* Spp. Enhances Host Susceptibility to Mucosal Inflammation. *Mucosal Immunol.* 2021, *14*, 113–124, doi:10.1038/s41385-020-0296-4.
49. MacCann, R.; Li, J.; Leon, A.A.G.; Negi, R.; Alalwan, D.; Tinago, W.; McGettrick, P.; Cotter, A.G.; Landay, A.; Sabin, C.; et al. Associations Between the Gut Microbiome, Inflammation, and Cardiovascular Profiles in People With Human Immunodeficiency Virus. *J. Infect. Dis.* 2025, *231*, e781–e791, doi:10.1093/infdis/jiaf043.
50. Allam, O.; Samarani, S.; Mehraj, V.; Jenabian, M.-A.; Tremblay, C.; Routy, J.-P.; Amre, D.; Ahmad, A. HIV Induces Production of IL-18 from Intestinal Epithelial Cells That Increases Intestinal Permeability and Microbial Translocation. *PLoS One* 2018, *13*, e0194185, doi:10.1371/journal.pone.0194185.
51. Ouyang, J.; Yan, J.; Zhou, X.; Isnard, S.; Harypursat, V.; Cui, H.; Routy, J.-P.; Chen, Y. Relevance of Biomarkers Indicating Gut Damage and Microbial Translocation in People Living with HIV. *Front. Immunol.* 2023, *14*, doi:10.3389/fimmu.2023.1173956.
52. Falasca, K.; Manigrasso, M.R.; Racciatti, D.; Zingariello, P.; Dalessandro, M.; Ucciferri, C.; Mancino, P.; Marinopiccoli, M.; Petrarca, C.; Conti, P.; et al. Associations between Hypertriglyceridemia and Serum Ghrelin, Adiponectin, and IL-18 Levels in HIV-Infected Patients. *Ann. Clin. Lab. Sci.* 2006, *36*, 59–66.
53. Hishiya, N.; Uno, K.; Nakano, A.; Konishi, M.; Higashi, S.; Eguchi, S.; Ariyoshi, T.; Matsumoto, A.; Oka, K.; Takahashi, M.; et al. Association between the Gut Microbiome and Organic Acid Profiles in a Japanese Population with HIV Infection. *Journal of Infection and Chemotherapy* 2024, *30*, 58–66, doi:10.1016/j.jiac.2023.09.013.
54. Narayanan, A.; Kieri, O.; Vesterbacka, J.; Manoharan, L.; Chen, P.; Ghorbani, M.; Ljunggren, H.-G.; Sällberg Chen, M.; Aleman, S.; Sönnernborg, A.; et al. Exploring the Interplay between Antiretroviral Therapy and the Gut-Oral Microbiome Axis in People Living with HIV. *Sci. Rep.* 2024, *14*, 17820, doi:10.1038/s41598-024-68479-4.
55. Mikaeloff, F.; Gelpi, M.; Benfeitas, R.; Knudsen, A.D.; Vestad, B.; Høgh, J.; Hov, J.R.; Benfield, T.; Murray, D.; Giske, C.G.; et al. Network-Based Multi-Omics Integration Reveals Metabolic at-Risk Profile within Treated HIV-Infection. *Elife* 2023, *12*, doi:10.7554/eLife.82785.
56. Hespell, R.B.; Paster, B.J.; Dewhirst, F.E. The Genus *Selenomonas*. In *Prokaryotes*; 2006; Vol. 4, pp. 982–990.
57. Li, Y.; Saxena, D.; Chen, Z.; Liu, G.; Abrams, W.R.; Phelan, J.A.; Norman, R.G.; Fisch, G.S.; Corby, P.M.; Dewhirst, F.; et al. HIV Infection and Microbial Diversity in Saliva. *J. Clin. Microbiol.* 2014, *52*, 1400–1411, doi:10.1128/JCM.02954-13.
58. Narayanan, A.; Kieri, O.; Vesterbacka, J.; Manoharan, L.; Chen, P.; Ghorbani, M.; Ljunggren, H.G.; Sällberg Chen, M.; Aleman, S.; Sönnernborg, A.; et al. Exploring the Interplay between Antiretroviral Therapy and the Gut-Oral Microbiome Axis in People Living with HIV. *Sci. Rep.* 2024, *14*, 1–10, doi:10.1038/s41598-024-68479-4.
59. Chen, Y.; Lin, H.; Cole, M.; Morris, A.; Martinson, J.; McKay, H.; Mimiaga, M.; Margolick, J.; Fitch, A.; Methe, B.; et al. Signature Changes in Gut Microbiome Are Associated with Increased Susceptibility to HIV-1 Infection in MSM. *Microbiome* 2021, *9*, 237, doi:10.1186/s40168-021-01168-w.

60. Ling, Z.; Jin, C.; Xie, T.; Cheng, Y.; Li, L.; Wu, N. Alterations in the Fecal Microbiota of Patients with HIV-1 Infection: An Observational Study in A Chinese Population. *Sci. Rep.* 2016, *6*, 30673, doi:10.1038/srep30673.
61. Cook, R.R.; Fulcher, J.A.; Tobin, N.H.; Li, F.; Lee, D.; Woodward, C.; Javanbakht, M.; Brookmeyer, R.; Shoptaw, S.; Bolan, R.; et al. Combined Effects of HIV and Obesity on the Gastrointestinal Microbiome of Young Men Who Have Sex with Men. *HIV Med.* 2020, *21*, 365–377, doi:10.1111/hiv.12838.
62. Louis, P.; Flint, H.J. Formation of Propionate and Butyrate by the Human Colonic Microbiota. *Environ. Microbiol.* 2017, *19*, 29–41, doi:10.1111/1462-2920.13589.
63. Louis, P.; Flint, H.J. Formation of Propionate and Butyrate by the Human Colonic Microbiota. *Environ. Microbiol.* 2017, *19*, 29–41, doi:10.1111/1462-2920.13589.
64. Van Hul, M.; Le Roy, T.; Prifti, E.; Dao, M.C.; Paquot, A.; Zucker, J.-D.; Delzenne, N.M.; Muccioli, G.G.; Clément, K.; Cani, P.D. From Correlation to Causality: The Case of *Subdoligranulum*. *Gut Microbes* 2020, *12*, 1849998, doi:10.1080/19490976.2020.1849998.
65. Zhernakova, A.; Kurilshikov, A.; Bonder, M.J.; Tigchelaar, E.F.; Schirmer, M.; Vatanen, T.; Mujagic, Z.; Vila, A.V.; Falony, G.; Vieira-Silva, S.; et al. Population-Based Metagenomics Analysis Reveals Markers for Gut Microbiome Composition and Diversity. *Science (1979)*. 2016, *352*, 565–569, doi:10.1126/science.aad3369.
66. Dillon, S.M.; Kibbie, J.; Lee, E.J.; Guo, K.; Santiago, M.L.; Austin, G.L.; Gianella, S.; Landay, A.L.; Donovan, A.M.; Frank, D.N.; et al. Low Abundance of Colonic Butyrate-Producing Bacteria in HIV Infection Is Associated with Microbial Translocation and Immune Activation. *AIDS* 2017, *31*, 511–521, doi:10.1097/QAD.0000000000001366.
67. Nowak, P.; Troseid, M.; Avershina, E.; Barqasho, B.; Neogi, U.; Holm, K.; Hov, J.R.; Noyan, K.; Vesterbacka, J.; Svärd, J.; et al. Gut Microbiota Diversity Predicts Immune Status in HIV-1 Infection. *AIDS* 2015, *29*, 2409–2418, doi:10.1097/QAD.0000000000000869.
68. Islam, S.M.S.; Singh, S.; Keshavarzian, A.; Abdel-Mohsen, M. Intestinal Microbiota and Aging in People with HIV—What We Know and What We Don't. *Curr. HIV/AIDS Rep.* 2025, *22*, 9, doi:10.1007/s11904-024-00717-w.
69. Singh, S.; Giron, L.B.; Shaikh, M.W.; Shankaran, S.; Engen, P.A.; Bogin, Z.R.; Bambi, S.A.; Goldman, A.R.; Azevedo, J.L.L.C.; Orgaz, L.; et al. Distinct Intestinal Microbial Signatures Linked to Accelerated Systemic and Intestinal Biological Aging. *Microbiome* 2024, *12*, 31, doi:10.1186/s40168-024-01758-4.
70. Toya, T.; Corban, M.T.; Marrietta, E.; Horwath, I.E.; Lerman, L.O.; Murray, J.A.; Lerman, A. Coronary Artery Disease Is Associated with an Altered Gut Microbiome Composition. *PLoS One* 2020, *15*, e0227147, doi:10.1371/journal.pone.0227147.
71. Gradisteanu Pircalabioru, G.; Liaw, J.; Gundogdu, O.; Corcionivoschi, N.; Ilie, I.; Oprea, L.; Musat, M.; Chifiriuc, M.-C. Effects of the Lipid Profile, Type 2 Diabetes and Medication on the Metabolic Syndrome—Associated Gut Microbiome. *Int. J. Mol. Sci.* 2022, *23*, 7509, doi:10.3390/ijms23147509.
72. Baltazar-Díaz, T.A.; González-Hernández, L.A.; Aldana-Ledesma, J.M.; Peña-Rodríguez, M.; Vega-Magaña, A.N.; Zepeda-Morales, A.S.M.; López-Roa, R.I.; del Toro-Arreola, S.; Martínez-López, E.; Salazar-Montes, A.M.; et al. Escherichia/Shigella, SCFAs, and Metabolic Pathways—The Triad That Orchestrates Intestinal Dysbiosis in Patients with Decompensated Alcoholic Cirrhosis from Western Mexico. *Microorganisms* 2022, *10*, 1231, doi:10.3390/microorganisms10061231.
73. Castaño-Jiménez, P.A.; Baltazar-Díaz, T.A.; González-Hernández, L.A.; García-Salcido, R.; Klimov-Kravtchenko, K.; Andrade-Villanueva, J.F.; Arellano-Arteaga, K.J.; Padilla-Sánchez, M.P.; Del Toro-Arreola, S.; Bueno-Topete, M.R. Deciphering the Language of Intestinal Microbiota Associated with Sepsis, Organ Failure, and Mortality in Patients with Alcohol-Related Acute-on-Chronic Liver Failure (ACLF): A Pioneer Study in Latin America. *Microorganisms* 2025, *13*, 1138, doi:10.3390/microorganisms13051138.
74. Van Hul, M.; Le Roy, T.; Prifti, E.; Dao, M.C.; Paquot, A.; Zucker, J.D.; Delzenne, N.M.; Muccioli, G.; Clément, K.; Cani, P.D. From Correlation to Causality: The Case of *Subdoligranulum*. *Gut Microbes* 2020, *12*, 1–13, doi:10.1080/19490976.2020.1849998.
75. Cani, P.D.; Amar, J.; Iglesias, M.A.; Poggi, M.; Knauf, C.; Bastelica, D.; Neyrinck, A.M.; Fava, F.; Tuohy, K.M.; Chabo, C.; et al. Metabolic Endotoxemia Initiates Obesity and Insulin Resistance. *Diabetes* 2007, *56*, 1761–1772, doi:10.2337/db06-1491.

76. Pedro, M.N.; Magro, D.O.; Da Silva, E.U.P.P.; Guadagnini, D.; Santos, A.; De Jesus Pedro, R.; Saad, M.J.A. Plasma Levels of Lipopolysaccharide Correlate with Insulin Resistance in HIV Patients. *Diabetol. Metab. Syndr.* 2018, *10*, 1–7, doi:10.1186/s13098-018-0308-7.
77. Koh, A.; Mannerås-Holm, L.; Yunn, N.-O.; Nilsson, P.M.; Ryu, S.H.; Molinaro, A.; Perkins, R.; Smith, J.G.; Bäckhed, F. Microbial Imidazole Propionate Affects Responses to Metformin through P38 $\gamma$ -Dependent Inhibitory AMPK Phosphorylation. *Cell Metab.* 2020, *32*, 643–653.e4, doi:10.1016/j.cmet.2020.07.012.
78. Molinaro, A.; Bel Lassen, P.; Henricsson, M.; Wu, H.; Adriouch, S.; Belda, E.; Chakaroun, R.; Nielsen, T.; Bergh, P.-O.; Rouault, C.; et al. Imidazole Propionate Is Increased in Diabetes and Associated with Dietary Patterns and Altered Microbial Ecology. *Nat. Commun.* 2020, *11*, 5881, doi:10.1038/s41467-020-19589-w.
79. Trøseid, M.; Nielsen, S.D.; Vujkovic-Cvijin, I. Gut Microbiome and Cardiometabolic Comorbidities in People Living with HIV. *Microbiome* 2024, *12*, 106, doi:10.1186/s40168-024-01815-y.
80. Koh, A.; Molinaro, A.; Ståhlman, M.; Khan, M.T.; Schmidt, C.; Mannerås-Holm, L.; Wu, H.; Carreras, A.; Jeong, H.; Olofsson, L.E.; et al. Microbially Produced Imidazole Propionate Impairs Insulin Signaling through MTORC1. *Cell* 2018, *175*, 947–961.e17, doi:10.1016/j.cell.2018.09.055.
81. Riggen-Bueno, V.; Del Toro-Arreola, S.; Baltazar-Díaz, T.A.; Vega-Magaña, A.N.; Peña-Rodríguez, M.; Castaño-Jiménez, P.A.; Sánchez-Orozco, L.V.; Vera-Cruz, J.M.; Bueno-Topete, M.R. Intestinal Dysbiosis in Subjects with Obesity from Western Mexico and Its Association with a Proinflammatory Profile and Disturbances of Folate (B9) and Carbohydrate Metabolism. *Metabolites* 2024, *14*, 121, doi:10.3390/metabo14020121.
82. De la Cuesta-Zuluaga, J.; Mueller, N.; Álvarez-Quintero, R.; Velásquez-Mejía, E.; Sierra, J.; Corrales-Agudelo, V.; Carmona, J.; Abad, J.; Escobar, J. Higher Fecal Short-Chain Fatty Acid Levels Are Associated with Gut Microbiome Dysbiosis, Obesity, Hypertension and Cardiometabolic Disease Risk Factors. *Nutrients* 2018, *11*, 51, doi:10.3390/nu11010051.
83. Chávez-Carbajal, A.; Nirmalkar, K.; Pérez-Lizaur, A.; Hernández-Quiroz, F.; Ramírez-Del-Alto, S.; García-Mena, J.; Hernández-Guerrero, C. Gut Microbiota and Predicted Metabolic Pathways in a Sample of Mexican Women Affected by Obesity and Obesity plus Metabolic Syndrome. *Int. J. Mol. Sci.* 2019, *20*, doi:10.3390/ijms20020438.
84. Kim, K.N.; Yao, Y.; Ju, S.Y. Short Chain Fatty Acids and Fecal Microbiota Abundance in Humans with Obesity: A Systematic Review and Meta-Analysis. *Nutrients* 2019, *11*, 2512, doi:10.3390/nu11102512.
85. Palmas, V.; Pisanu, S.; Madau, V.; Casula, E.; Deledda, A.; Cusano, R.; Uva, P.; Vascellari, S.; Loviselli, A.; Manzin, A.; et al. Gut Microbiota Markers Associated with Obesity and Overweight in Italian Adults. *Sci. Rep.* 2021, *11*, doi:10.1038/s41598-021-84928-w.
86. Pluznick, J.L.; Protzko, R.J.; Gevorgyan, H.; Peterlin, Z.; Sipos, A.; Han, J.; Brunet, I.; Wan, L.-X.; Rey, F.; Wang, T.; et al. Olfactory Receptor Responding to Gut Microbiota-Derived Signals Plays a Role in Renin Secretion and Blood Pressure Regulation. *Proceedings of the National Academy of Sciences* 2013, *110*, 4410–4415, doi:10.1073/pnas.1215927110.
87. Wei, Y.; Ma, X.; Zhao, J.; Wang, X.; Gao, C. Succinate Metabolism and Its Regulation of Host-Microbe Interactions. *Gut Microbes* 2023, *15*, doi:10.1080/19490976.2023.2190300.
88. Konstanti, P.; Gómez-Martínez, C.; Muralidharan, J.; Vioque, J.; Corella, D.; Fitó, M.; Vidal, J.; Tinahones, F.J.; Torres-Collado, L.; Coltell, O.; et al. Faecal Microbiota Composition and Impulsivity in a Cohort of Older Adults with Metabolic Syndrome. *Sci. Rep.* 2024, *14*, 28075, doi:10.1038/s41598-024-78527-8.
89. Gradisteanu Pircalabioru, G.; Liaw, J.; Gundogdu, O.; Corcionivoschi, N.; Ilie, I.; Oprea, L.; Musat, M.; Chifiriuc, M.-C. Effects of the Lipid Profile, Type 2 Diabetes and Medication on the Metabolic Syndrome—Associated Gut Microbiome. *Int. J. Mol. Sci.* 2022, *23*, 7509, doi:10.3390/ijms23147509.

**Disclaimer/Publisher's Note:** The statements, opinions and data contained in all publications are solely those of the individual author(s) and contributor(s) and not of MDPI and/or the editor(s). MDPI and/or the editor(s) disclaim responsibility for any injury to people or property resulting from any ideas, methods, instructions or products referred to in the content.